Measurements of screening length in salt solutions by Total Internal Reflection Microscopy: influence of van der Waals forces and instrumental noise

M. Nayeri, Z. Abbas, J. Bergenholtz*

Department of Chemistry and Molecular Biology, University of Gothenburg, Kemivägen 10, SE-412 96 Göteborg, Sweden

Abstract

Total internal reflection microscopy (TIRM) measurements of colloidal spheres in aqueous electrolyte solutions have been carried out with focus on screening properties of various electrolytes and methods and analyses for reliably extracting them from TIRM measurements. Approximations based on Lifshitz theory of flat plates are found to yield van der Waals interactions that are too strong compared to measured interaction potentials. Allowing for some attenuation of these interactions due to surface roughness, a consistent set of screening lengths can be extracted by fitting a model of the interaction, comprising screened Coulomb, van der Waals, and gravitational interactions, to the TIRM data. With the exception of the 2:2 electrolytes, the screening lengths extracted from the TIRM measurements are well described by Debye-Hückel theory, including some surfactants below their critical micelle concentration and electrolytes with large size asymmetries between anion and cation. In 2:2 electrolytes the screening lengths are found to be larger than the corresponding Debye length by as much as 50% at the highest salt concentrations studied. While this deviation is significantly larger than predictions of theory based on the primitive model of electrolytes, similar magnitudes are found from analysis of BD simulations with added noise at realistic levels in the incident intensity. The work shows that care has to be taken when extracting parameters governing potentials in the presence of noise, particularly at high ionic strengths when potentials become steep at short separations.

Keywords: Total internal reflection microscopy, latex, electrolyte, screening, van der Waals interactions, electrostatic interaction, interaction potential, noise, Brownian dynamics, computer simulation

1. Introduction

The electrostatic interaction is an important part of the total interaction free energy that usually influences the properties of dispersions of colloidal particles very strongly [1]. This interaction is also known as the electrical double-layer (EDL) interaction where the name refers to the charged surface and the surrounding diffuse layer of counterions and coions that serves to stabilize particles against aggregation. A repulsive interaction arises between two charged surfaces with uniform surface charge of the same sign or a charged surface and a neutral surface when the diffuse layer starts to overlap with either the diffuse layer of the other charged sur-

*Author to whom correspondence should be addressed

Email address: jbergen@chem.gu.se (M. Nayeri, Z. Abbas, J. Bergenholtz)

face or when it is compressed by the uncharged surface [2], at least if the electrostatic coupling is not too strong [3]. The thickness of the diffuse layer and its screening of the surface charge depend greatly on the concentration and valence of the ions in the solution. In the classical Gouy-Chapman theory of the EDL interaction that forms part of the Derjaguin-Landau-Verwey-Overbeek (DLVO) theory of colloidal stability, the force between charged surfaces decays exponentially at sufficiently large separations with a decay length given by the Debye-Hückel (DH) screening length, κ^{-1}, where $\kappa^2 = \sum_j \frac{(z_j e)^2 n_j}{\varepsilon_r \varepsilon_0 k_B T}$ is given in terms of the valence z_j and number density n_j of the j-th ionic species, respectively, with ε_r the dielectric constant of the solvent, ε_0 the permittivity of vacuum, and $k_B T$ the thermal energy. The degree of screening is well described by this expression for monovalent salts at low ionic strengths.

Direct measurements of interactions relevant to colloidal particles are possible with a few well-established techniques, such as the Surface Forces Apparatus (SFA) [4–8] and Atomic Force Microscopy (AFM) devices [9]. Another technique is Total Internal Reflection Microscopy (TIRM) [10–13], which allows for determination of particle-plane wall interaction potentials by recording the scattered intensity from a colloidal sphere illuminated by an evanescent field. It is ideally suited to detecting the weak interactions (of order $k_B T$) most relevant to colloidal stability [12]. Due to these techniques, the inversion of data for some measured property of the system can be avoided when determining parameters characterizing the interaction. For instance, for low ionic strengths, when the double layer extends to distances where the van der Waals interaction is negligible, this provides an unambiguous way of determining the screening length [4, 13]. In many situations multivalent rather than monovalent electrolytes are better suited to the purposes at hand, either because they provide more efficient screening of the EDL interaction or they modify the surface charge through adsorption or provide binding between molecules. With regard to the former, for higher electrolyte concentrations, and particularly for multivalent electrolyte, deviations from the Debye length is expected from theory [14–18] and such systematic deviations have been reported for some asymmetric electrolytes based on SFA measurements [4].

At higher ionic strengths the range of the electrostatic and van der Waals interactions can be of comparable magnitude and it becomes necessary to disentangle them in order to determine one or the other, which can be difficult [19]. In such a situation, Bevan and Prieve [20], for example, found significantly reduced screening lengths compared to those from the Debye-Hückel formula for monovalent electrolyte using TIRM and extracted van der Waals interactions that were considerably weaker than expected. In contrast, Helden et al. [21] and Ao et al. [22] found screening lengths in a similar concentration regime that were significantly larger than the calculated Debye lengths. These TIRM results, although at odds with one another, would seem to suggest that ions cannot be treated as simple point ions. Two complications arise when analyzing data from TIRM measurements at high ionic strengths. First, as already mentioned, the analysis necessarily becomes more complicated because the van der Waals interaction cannot be neglected. Second, the resulting interaction potentials become very steep and one might question whether such steep potentials can be accurately determined using TIRM measurements. After all, there are other sources of noise than that due to the Brownian motion of the particle which is recorded during the

measurement.

Against this background we set out to clarify the situation regarding screening effects in electrolyte solutions at higher than 1 mM ionic strengths as determined by TIRM. We conduct a systematic study of electrostatic and van der Waals interactions using TIRM, in which we include 1:1, 2:1, 1:2, 2:2, 3:1, and 3:2 salts and 1:1 and 2:1 surfactants. The study is further motivated by recent work with TIRM that suggests that ion specificity can be observed for 1:1 salts, especially anion specificity, at ionic strengths below 10 mM [22]. For this reason salts that deviate strongly from ideal behavior have been selected to ascertain whether such deviations affect the screening lengths as has been suggested in the past [23]. Additional motivation comes from the fact that TIRM has not been used to examine systematically the screening due to multivalent ions. The screening properties are investigated for solutions of NaCl, tetrabutyl ammonium fluoride (TBAF), tetrabutyl ammonium iodide (TBAI), Na_2SO_4, sodium dodecylsulfate (SDS), magnesium dodecylsulfate ($Mg(DS)_2$), $MgSO_4$, $ZnSO_4$, $AlNO_3$, and $Al_2(SO_4)_3$. In brief, the work shows that, with the exception of 2:2 electrolytes, the DH formula captures the screening at sub-mM ionic strengths and also up to 1-2 mM ionic strengths provided some weakening of the van der Waals interaction, presumably due to surface roughness, is allowed for. At higher ionic strengths the TIRM measurements become prone to distortions by noise and to extract precise screening lengths at ionic strengths in excess of a few mM requires special precautions to limit noise.

2. Material and methods

2.1. TIRM Measurements

The experimental results were obtained using an in-house TIRM setup that has been described in an earlier publication [24]. For a more detailed description of TIRM functionality, readers are referred to reviews regarding the TIRM setup [11, 12, 25]. In brief, in TIRM light scattered from a single spherical colloidal particle illuminated by an evanescent field is measured. Following some precautions [26, 27], one can relate the scattered intensity to the distance between the colloidal sphere and the surface from where the evanescent wave originates as

$$I(h) = I_0 \exp(-\zeta h) \tag{1}$$

where $I(h)$ is the scattering from the particle at vertical position h, ζ^{-1} is the decay length of the evanescent field, and I_0 is the maximum scattering intensity of the particle when attached to the surface at $h = 0$. Measuring the distance between the colloidal particle and the surface over a long period of time allows for a histogram to be constructed for the positions that the particle samples in the vertical direction. Using the Boltzmann distribution,

$$p(h) \propto \exp\left(\frac{-\phi(h)}{k_B T}\right), \tag{2}$$

the probability function $p(h)$ of finding a particle at a certain distance h from the surface is transformed to the potential energy as a function of the distance $\phi(h)$. In practice intensity histograms are constructed, which can be related to $p(h)$ [12]. These comprised at least 10^5 data points, with intensities recorded at 10 ms time intervals.

2.2. Brownian dynamics simulations of TIRM measurements

To assess the influence of noise on TIRM measurements, we follow Sholl et al. [28] and conduct Brownian dynamics (BD) simulations of a sphere in Brownian motion perpendicular to a plane wall. Briefly, in the BD algorithm the particle-plane wall separations are updated following

$$h(t + \Delta t) = h(t) + \left(\frac{dD}{dh} + \frac{D}{k_B T}F\right)\Delta t + H(\Delta t) \quad (3)$$

where Δt is the time step and $H(\Delta t)$ is a random displacement, drawn from a Gaussian distribution, fulfilling $\langle H \rangle = 0$ and $\langle H^2 \rangle = 2D\Delta t$. The diffusion coefficient D depends on the height above the plane wall and is approximated by $D(x)/D_0 = (6x^2 + 2x)/(6x^2 + 9x + 2)$, where $x = h/a$ and a is the sphere radius [29]. The elevations sampled by a 5 μm radius polystyrene sphere subject to a force law $F = -\frac{d\phi}{dh}$ comprising only electrostatic and gravitational contributions were simulated using Eq. 3 with Δt =0.1 ms and the intensity was determined every ms from this BD trajectory using Eq. 1 with ζ^{-1} as in the actual measurements. Surface potentials of -40 mV were used for both the particle and glass wall and the expression given by Prieve [12] for the electrostatic prefactor B was used. Gaussian white noise with zero mean and varying standard deviation σ was added to this intensity. The elevations were assembled into a histogram using a resolution in separation distance of Δh = 0.4 nm and the potential was extracted using Eq. 2. To isolate the effect of noise on the TIRM analysis, data from very long trajectories, corresponding to 1400-minute runs, were collected.

2.3. Sample preparation

Laser light with a wavelength of 658 nm was totally reflected at an angle of incidence of 72 degrees, using a dovetail prism of the same angle, giving a decay length ζ^{-1} of about 93 nm for the evanescent field [12]. The prism was optically coupled to a microscope slide (Gerhard Meltzer, refractive index=1.517) at the bottom of the measuring cell, using an optically matched immersion oil (Carl Zeiss, refractive index=1.518). In most of the measurements spherical polystyrene particles with nominal diameters of 10.0 ± 0.4 μm (Polysciencs Inc.) were used. For measurements in aqueous solutions of $Al_2(SO_4)_3$, silica particles (Fluka) with a nominal diameter of 5.0 ±0.3 μm were used. The stock solutions contained 2.5 wt. % and 5 wt. % polystyrene and silica particles, respectively. Since TIRM operates on single particles, it is necessary to ensure that very few particles enter the TIRM cell. One drop of particle stock solution was highly diluted with the lowest concentration of the salt solution to be measured on by adding a drop of stock dispersion to an equivalent of about 100 L. All the salts used, besides $Mg(DS)_2$, were purchased with a purity of at least ≥99.5 % and used without further purification. $Mg(DS)_2$ was prepared according to the procedure suggested by Maciejewska *et al.* [30], in which $MgCl_2$ is added in 20% stoichiometric excess to a SDS solution. This leads to precipitation of $Mg(DS)_2$. The supernatant was then replaced with Milli-Q water (18 MΩ·cm). The supernatant replacement was repeated several times so as to remove the sodium and chloride ions. The precipitate was subsequently vacuum dried at 40°C. All salt solutions were prepared using Milli-Q grade water. Measurements at different salt concentrations were performed by adding aliquots of concentrated salt solution to a Teflon flask reservoir connected to the measuring cell, followed by pumping the solutions around a closed circuit in order to homogenize the ionic strength while keeping the colloidal particle selected for the measure-

ment in place with an optical tweezer.

3. Results and discussion

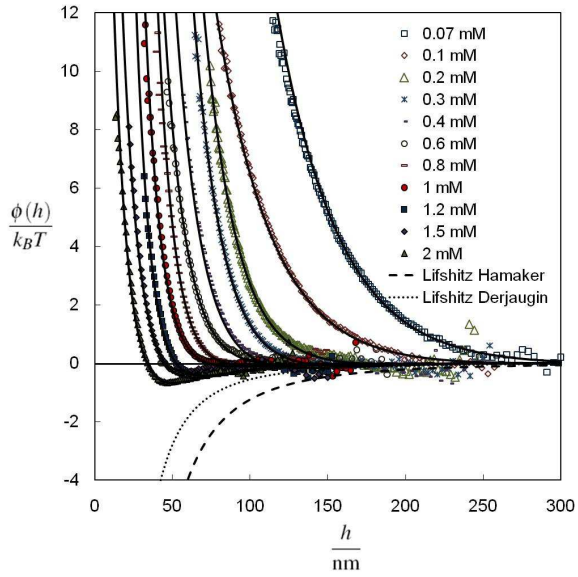

Figure 1: Measurement series of interaction energy as a function of separation distance and concentration of the organic salt TBAI. The solid lines are fits as described in the text. Also, shown for comparison, following Bevan and Prieve [20], are the results of calculating the van der Waals interaction using Lifshitz theory for two smooth glass and polystyrene surfaces in 1 mM 1:1 salt and combining it with Hamaker's expression for the sphere-wall interaction in Eq. 4 and Derjaguin's approximation in Eq. 5.

In Fig. 1 the normalized interaction energy for a polystyrene particle above a plane glass wall is shown as a function of surface-surface separation and concentration of the monovalent salt TBAI. The effect of gravity has been subtracted, leaving the electrostatic and van der Waals interactions, and the curves have been shifted such that the interaction potential vanishes in the limit of large distances. The same particle was used for all the ionic strengths shown. As seen, the interaction is predominantly repulsive. At low salt concentrations this repulsion extends relatively large distances and with increasing salt concentration the range of the repulsion is progressively shortened. At salt concentrations in excess of 1 mM an attraction also appears and at sufficiently high salt concentrations the particle becomes attached to the glass surface. All these features are qualitatively consistent with what is expected based on DLVO theory. However, in attempts to model the data quantitatively, it immediately becomes apparent that the magnitude of the van der Waals interaction is significantly reduced relative to what one might expect from theory. The following two expressions used by Bevan and Prieve [20] for the van der Waals interaction have been employed

$$\phi_{\mathrm{vdW}}(h) = -\frac{A(h)}{6}\left(\frac{2a}{h}\frac{h+a}{h+2a} - \ln\frac{h+2a}{h}\right) \quad (4)$$

$$\phi_{\mathrm{vdW}}(h) = -2\pi a\int_h^\infty \frac{A(h')}{12\pi h'^2}dh' \quad (5)$$

where $A(h)$ is the Hamaker function from Lifshitz theory for flat plates. In Eq. 4 the plane wall-sphere Hamaker expression is used but with the Hamaker constant replaced by the Hamaker function from Lifshitz theory for flat plates, an approximation suggested by Mahanty and Ninham [31], which has been tested for the sphere-sphere geometry [32, 33]. Equation 5 is Derjaguin's approximation, which is expected to hold in the limit of small separation distances. The results for polystyrene interacting with glass across a 1 mM 1:1 salt solution have been included in Fig. 1. The effects of screening and retardation have been accounted for in the same manner as done by Bevan and Prieve [20]. In agreement with their observations, Fig. 1 shows that Eqs. 4 and 5 significantly overpredict the strength of the van der Waals interaction and cannot be used to analyze the TIRM data. This is particularly apparent at the higher salt concentrations in Fig. 1 where a clear sec-

ondary DLVO-like minimum develops, the shallowness of which is not captured by either of Eqs. 4 or 5. Similar findings have been made by Prieve et al. [20, 34] and by Walz et al. [35, 36]. Both groups have suggested that surface roughness on the particle and glass wall are the cause of the attenuation of the van der Waals interaction seen in the TIRM measurements.

3.1. Model for the interaction potential

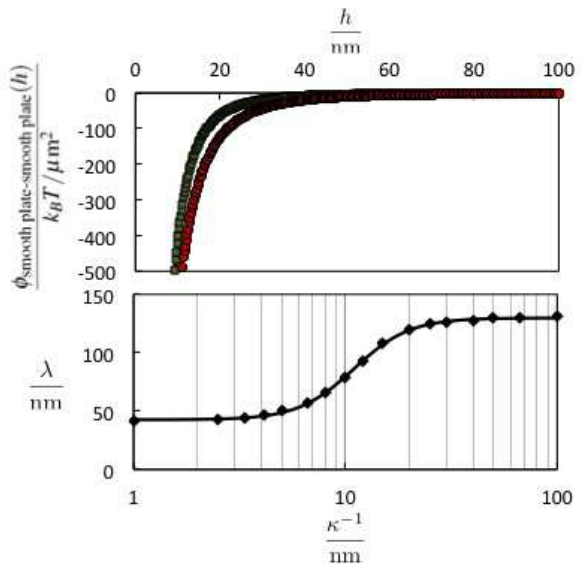

Figure 2: Top panel: The lines show results of Lifshitz theory for flat plates, with a screened zero-frequency term [20, 31], for two different salt concentrations corresponding to Debye lengths of 100 nm and 5 nm. The circles show the fit of the retarded Hamaker theory in Eq. 6, which yields $\lambda = 131$ nm for a Debye length of 100 nm, while the squares produce $\lambda = 50$ nm for a Debye length of 5 nm. In both cases the Hamaker constant in Eq. 6 was set to $3\,k_BT$. Bottom panel: Interaction wavelength λ in Eq. 6 as a function of Debye length with the correlation in Eq. 7 as the solid line.

The finding of weaker van der Waals interactions than produced by Lifshitz theory is in agreement with observations made in past TIRM studies [20, 35] and necessitates identifying an alternative approach to handling the van der Waals interaction. The discrepancy has been attributed to surface roughness [20, 35] and a number of ways have been devised to account for the effect of surface roughness on van der Waals interactions [34, 37, 38]. Walz and co-workers [35, 36, 38] modeled the roughness by adding hemispherical asperities uniformly to otherwise smooth surfaces using a retarded Hamaker approach, which we apply because the final expressions are analytical and are well suited to analysis of TIRM data. Expressions for van der Waals interaction energies have been derived assuming pair-wise additivity of retarded molecular interactions [39, 40] in an approach very similar to Hamaker's for non-retarded interactions [41]. This procedure produces the following interaction energy per area for flat plates [38, 39]

$$\frac{\phi(h)}{\text{area}} = -A\left(\frac{2.45\lambda}{60\pi^2h^3} - \frac{2.17\lambda^2}{240\pi^3h^4} + \frac{0.59\lambda^3}{840\pi^4h^5}\right) \quad (6)$$

where λ is a characteristic wavelength of the interaction. Rather than setting this wavelength to some *a priori* value, e.g. 100 nm, as is usually done [39, 40], it is determined here in the way suggested by Suresh and Walz [35], through comparison with the Lifshitz theory for flat plates using polystyrene interacting with polystyrene across aqueous salt solutions. Values for λ were determined in this way as a function of the Debye length based on least squares fits of Eq. 6 to Lifshitz theory. The resulting relation between λ and κ^{-1} is well represented by

$$\frac{\lambda}{\text{nm}} = 86.2 + 43.6\tanh\left[3.8(\log_{10}\kappa^{-1} - 1.04)\right] \quad (7)$$

which is shown in Fig. 2.

As seen from the results in Fig. 2, screening of the static part of the van der Waals interaction [20, 31] alters the interaction significantly in going from Debye lengths of 5 to 100 nm. By using the different λ values from Eq. 7 one can account approximately for both

screening and retardation. Moreover, one confirms the presumption expressed by Suresh and Walz [38] that screening reduces the value of λ considerably below the 100 nm often used; Eq. 7 yields λ values of about 130 nm under low-salt conditions and 42.6 at high ionic strengths. Using the same retarded Hamaker approach, Czarnecki and Dabros [42] obtained the following expression for the van der Waals interaction between a smooth sphere of radius a and a semi-infinite flat wall

$$\begin{aligned}\phi_{\mathrm{vdW}}(h) &= A\left\{\frac{2.45\lambda}{60\pi}\left(\frac{h-a}{h^2}-\frac{h+3a}{(h+2a)^2}\right)\right. \\ &-\frac{2.17\lambda^2}{720\pi^2}\left(\frac{h-2a}{h^3}-\frac{h+4a}{(h+2a)^3}\right) \\ &\left.+\frac{0.59\lambda^3}{5040\pi^3}\left(\frac{h-3a}{h^4}-\frac{h+5a}{(h+2a)^4}\right)\right\}\end{aligned} \quad (8)$$

which is the geometry of interest for the TIRM measurements. We deviate somewhat from the procedure of Suresh and Walz and refrain from invoking the Derjaguin approximation altogether and add instead this expression to theirs for the asperity interaction with the flat plate [38]. In the modeling of the TIRM data setting the asperity radius to 30 nm and the surface coverage to 10%, which is within the set of values that Suresh and Walz found to agree best with their experimental results [35], allows for modeling the TIRM data with reasonable values for the Hamaker constant. The Hamaker constant in Eq. 8 was obtained by regression against the TIRM data.

To analyze the TIRM measurements of interaction potentials in electrolyte solutions, in addition to the van der Waals interaction $\phi_{\mathrm{vdW}}(h)$, the following contributions to the colloidal sphere-plane wall interaction are considered,

$$\phi(h) = \phi_G(h) + \phi_{\mathrm{el}}(h) + \phi_{\mathrm{vdW}}(h) \quad (9)$$

where $\phi_G(h)$ is the gravitational potential energy and $\phi_{\mathrm{el}}(h)$ is the EDL repulsion. The expression for the gravitational potential comes from the buoyant weight of the colloidal particle; in the fits of the data, since the same particle was used for measurements at different ionic strengths, the particle diameter was allowed to vary by at most ±2 % for a given series of ionic strengths. Linear superposition with Derjaguin's approximation, resulting in $\phi_{\mathrm{el}}(h) = B\exp(-\kappa h)$, has been shown to model the EDL interaction energy well under conditions typical for TIRM [10, 13]. The prefactor B contains information on the surface potentials of the colloidal sphere and the glass plate and its value is strongly correlated with the most-sampled distance between the particle and the plane wall h_m [12]. The value of B is allowed to vary freely in the fitting process. The precise value of h_m requires measuring I_0 in Eq. 1, which is accomplished by conducting an intensity measurement with the particle attached to the glass wall at the end of each measurement series [12].

In summary, Eq. 9 was fitted to the experimental data by allowing the electrostatic prefactor, B, and the screening length, κ^{-1}, to vary freely. The Hamaker constant, A, was constrained to assume values between 1 and 3 k_BT and the particle diameter was allowed to vary by at most 2% across a full concentration series of the same salt for which the same particle was used. The Hamaker constants obtained from the fitting procedure varied by at most 1.2 and 2.8 k_BT within a concentration series of salt without any clear trend. Constraining the Hamaker constants further resulted in a gradual deterioration of the model fits, though without systematically affecting the screening lengths. For a given salt concentration series the electrostatic prefactor decreased, for the most part systematically, with increasing salt concentration. The values for B varied greatly, from $O(10^3)$

k_BT at low salt concentrations to $O(10)$ k_BT at high salt concentrations, but the values were within the range of those obtained by von Grünberg and co-workers [13] who explored also much lower salt concentrations.

3.2. Screening lengths

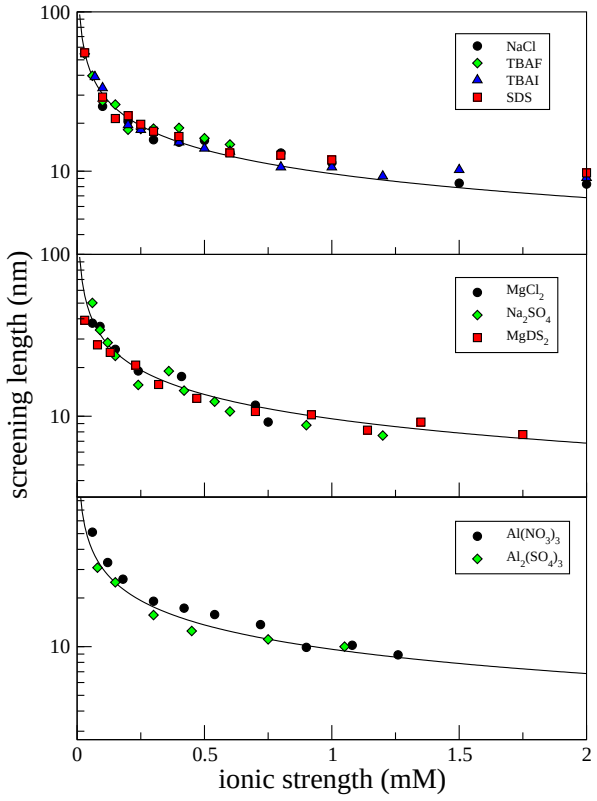

Figure 3: Screening lengths obtained from fits of Eq. 9 to TIRM data for a series of 1:1 salts (as labeled, top panel), 2:1 and 1:2 salts (as labeled, middle panel), and 3:1 and 3:2 salts (as labeled, bottom panel), as a function of ionic strength. The solid lines show the corresponding Debye length.

For measurements of particles suspended in solutions of lower salt concentrations the TIRM data are readily fit to the model in Eq. 9 as the longer screening length keeps the particle far from the plane glass wall and the contribution of the van der Waals interaction is negligible. At higher salt concentrations the particle comes sufficiently close to the surface that the inclusion and treatment of the van der Waals interaction becomes important; if it is left out the particle's buoyant weight would seem to acquire a dependence on the ionic strength [43]. It is for such situations, when the separation distance is only 3-5 times the screening length, that Bevan and Prieve extracted screening lengths for 1:1 electrolyte solutions that were only about half the value of the Debye length [20] whereas Helden et al. [21] and Ao et al. [22] in a similar concentration regime found screening lengths that were significantly larger than the ones from the DH formula. While deviations from the DH value may be expected for high electrolyte concentrations and/or multivalent electrolyte, theory suggests that in this concentration regime of 1:1 electrolytes the screening should be well captured by the DH expression [14–18].

Figure 1 shows the TIRM measurements of a particle suspended in solutions of the organic salt TBAI. This particular salt was selected because of the large size asymmetry between the anion and cation and because it deviates from ideal behavior in the opposite way of TBAF [44, 45], the screening properties of which was also determined by TIRM measurements. However, as summarized in Fig. 3 for a number of 1:1 electrolyte systems, no systematic trends can be observed in the extracted screening lengths; they all follow the DH result well. In all cases except for SDS, the particle could be irreversibly attached to the surface by adding enough electrolyte. The measurements in SDS solutions could be extended to higher concentrations than those shown in Fig. 3, exceeding the critical micelle concentration (CMC) of about 8 mM [24], probably due to adsorption of dodecyl sulfate molecules on the glass and particle surfaces. In this case both the most-sampled position of the particle as well as the fitted screening

length did not change much with increasing SDS concentration, giving a value of ~9 nm for the screening length at a concentration of 6 mM, which is about a factor of two greater than the expected 4 nm based on the DH formula. Such a saturation of the screening length with increasing concentration of SDS has been observed in colloidal probe-AFM measurements near and beyond the CMC [23]. However, below the CMC, SDS acts like a simple 1:1 electrolyte as also observed for other surfactants [7]. The agreement between the screening length determined by fitting the TIRM data and the DH result is good with deviations for the most part within 2 nm, which is the reproducibility as indicated by analysis of block-averaged data from the same particle. Even though we were unable to reach the 10 mM ionic strengths Ao and co-workers [22] managed to conduct measurements in, we certainly observe far less deviation from DH behavior than they did. The results for the screening length for TBAF solutions in Fig. 3 does not change much between 0.2 and 0.4 mM, which is something that occurs on occasion and is perhaps caused by the particle shifting position slightly.

Figure 3 also shows results for the screening lengths in 2:1 and 1:2 electrolytes, i.e. both with a divalent counterion and coion with respect to the negatively charged surfaces in contact with the electrolyte solution. Because of the higher valence TIRM measurements can only be conducted at lower salt concentrations compared to those for the monovalent electrolyte. As with SDS, $Mg(DS)_2$ comprises an exception and measurements in $Mg(DS)_2$ solutions could be conducted at high ionic strengths and particles in these surfactant solutions could not be irreversibly attached to the glass surface. The screening length exhibited the same saturation behavior above the CMC of 0.8 mM. Introducing the ionic strength $\mathcal{I}$ viz. $\kappa^2 = 2e^2\mathcal{I}/(\epsilon_r\epsilon_0 k_B T)$ and $\mathcal{I} = (1/2)\sum_j z_j^2 n_j$ allows for adopting a common concentration scale for the different electrolytes in Fig. 3. Again, the measured screening lengths are in agreement with the Debye length, which is consistent with SFA results on 2:1 electrolytes [5, 46].

Two further asymmetric electrolytes were investigated in the same manner. Fig. 3 shows the screening lengths in solutions of the 3:1 salt $Al(NO_3)_3$ and the 3:2 salt $Al_2(SO_4)_3$. The salt concentrations in these cases are restricted to $\lesssim$ 0.2 mM and $\lesssim$ 0.07 mM, respectively. In the former case a polystyrene particle was used whereas in the latter a silica particle was used in the TIRM measurements. The reason for this is that AFM measurements with a colloidal silica probe particle have yielded increased repulsions with increasing $Al_2(SO_4)_3$ concentration [47]. In the TIRM measurements no such trend is observed; rather, the screening length in Fig. 3 closely follows the DH formula for 3:2 electrolytes, suggesting complete dissociation into tri- and divalent ions. However, it should be noted that $Al_2(SO_4)_3$ dissolved in water acts as a weak acid with three different pKa values [48]. This gives a pH of around 4.5 at the concentrations the measurements in Fig. 3 were conducted at, which indeed should correspond to dissociated Al^{3+} and SO_4^{2-}. Above a pH of 5.5 it is known that precipitation starts in $Al_2(SO_4)_3$ solutions [48]. On increasing the pH by adding NaOH solution large precipitates formed, which settled at the bottom of the TIRM cell and hindered the silica sphere from coming close to the surface. This behavior likely explains the results reported by Donose et al. [47], and it is in accordance with the explanation they offered for the observed results. TIRM measurements of a polystyrene particle in solutions of the 3:1 salt $Al(NO_3)_3$, which is shown in Fig. 3, yields

screening lengths in good agreement with the DH result. Pashley [6] has made similar observations for 3:1 electrolytes using the SFA, but only once the trivalent cation had adsorbed on the strongly charged mica surfaces leading to reversal of the surface charge.

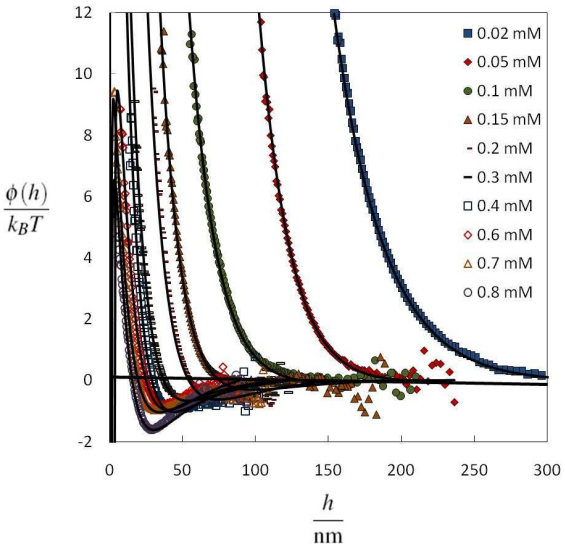

Figure 4: Measurement series of interaction energy as a function of separation distance and concentration of the 2:2 salt $MgSO_4$. The solid lines are fits as described in the text.

The screening in solutions of 2:2 salts has been examined as well. Figure 4 shows the TIRM measurements of a polystyrene particle suspended in $MgSO_4$ solutions of varying concentration of the salt. An attractive regime in the interaction sets in beyond 0.1 mM, which is a salt concentration that is roughly a factor of 5-10 lower than that seen for 1:1 electrolytes. The results have been fitted with Eq. 9, which suggests that the repulsive maximum in the DLVO interaction is below 10 k_BT for the highest salt concentrations. Indeed, the particle became attached to the glass wall at a $MgSO_4$ concentration just in excess of 0.8 mM.

The results for the screening length extracted from the fits of the TIRM data are shown in Fig. 5 for the 2:2

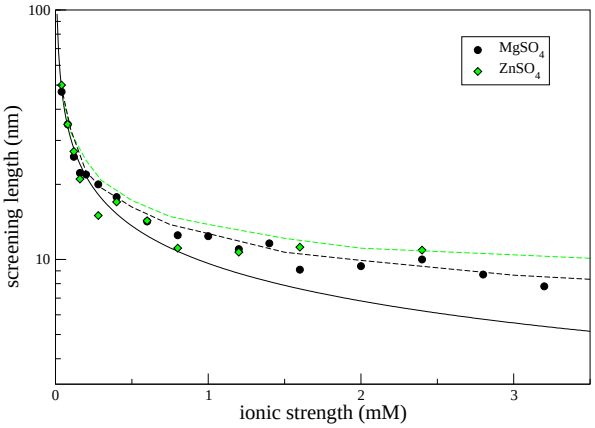

Figure 5: Screening lengths extracted from TIRM data for the 2:2 salts $MgSO_4$ and $ZnSO_4$. The solid line shows the corresponding Debye-Hückel screening length and the dashed lines derive from analysis of Brownian dynamics simulations with added noise levels of 5% and 4% of the mean incident intensity (see text and Fig. 7).

salts $MgSO_4$ and $ZnSO_4$. Whereas the screening lengths for all the other salts studied, including some surfactant solutions below their CMCs, were all in agreement with the Debye length, Fig. 5 shows screening lengths clearly greater than the Debye length. This holds for both 2:2 salts studied and similar deviations might have appeared for the other salts had we been able to investigate a similar range of ionic strength as in Fig. 5. Since it is known that symmetric multivalent ions exhibit a particularly strong tendency to associate and show large deviations from ideal behavior, it is tempting to ascribe the deviation from the DH formula in Fig. 5 to a break-down of the point ion assumption. Kjellander and Mitchell [15] carried the analysis of Mitchell and Ninham [14] a step further and obtained the leading-order correction to the Debye length for symmetric electrolytes. While in qualitative agreement with the positive deviation from the Debye length seen in Fig. 5, their analytical formula only yields a 5% increase in the screening length compared to the Debye length at the highest ionic strength in

Fig. 5. Monte Carlo simulations [49] and integral equation theory [50] corroborate this rather small deviation from DH theory in the concentration range studied in the TIRM measurements and it follows that we cannot reconcile the magnitude of the deviation from the Debye length in Fig. 5 with theory based on the primitive model. As an alternative we consider the role of noise in TIRM measurements at higher ionic strengths.

3.3. *Effect of noise*

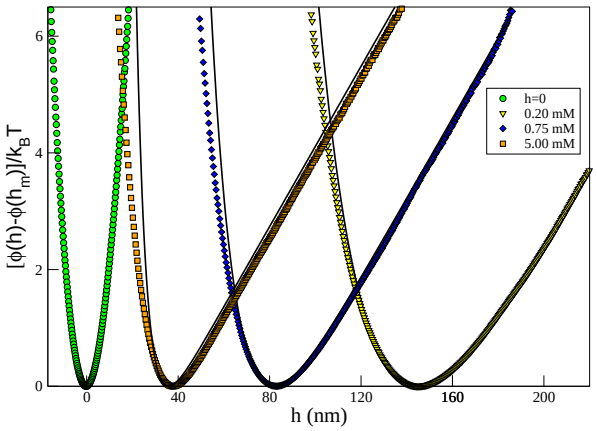

Figure 6: Potentials as a function of ionic strength extracted from BD simulations of a 5 μm polystyrene sphere polluted by Gaussian white noise in the incident intensity, characterized by a standard deviation $\sigma/I_0 = 0.05$, as labeled. The solid lines correspond to the true potential used in the BD simulations. The potential centered on $h = 0$ corresponds to a particle stuck to the glass wall. The range used for fitting the potentials shown from the BD simulations was restricted to a maximum of 6.5 k_BT.

Experimental noise is known to affect the potentials extracted from TIRM measurements. Prieve and coworkers examined both how additive background noise [28, 51] and how noise in the incident intensity [28] affects the TIRM analysis for particles at moderate ionic strengths. In the following we investigate how noise distorts potentials at the high ionic strengths where we observe deviations in extracted screening lengths from the expected Debye lengths. To this end, we use the Brownian dynamics simulation technique developed for TIRM by Sholl et al. [28], which generates separation distances or elevations of a particle diffusing near a plane wall in a force field that is known exactly. From the particle positions ideal intensities can be calculated using Eq. 1. These intensities are then corrupted by adding noise, which leads to some degree of distortion in the extracted potential.

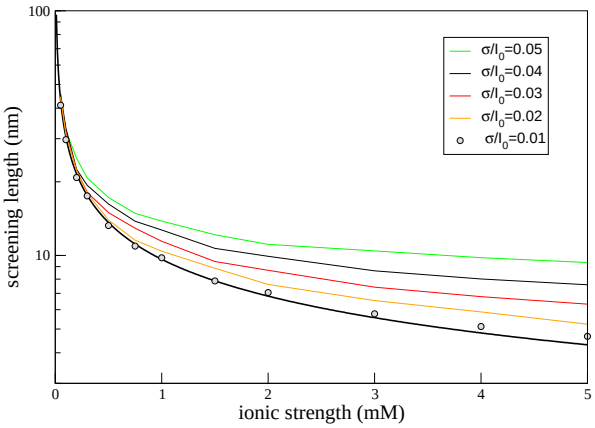

Figure 7: Screening lengths as a function of ionic strength extracted from BD simulations of a 5 μm polystyrene sphere polluted by Gaussian white noise in the incident intensity characterized by a standard deviation σ and incident intensity I_0, as labeled. The bottom-most solid line is the Debye length used in the BD simulations.

In the TIRM set-up used here the incident laser light is focused on the particle in the TIRM cell in order to improve the signal-to-noise ratio by limiting scattering from other sources than the particle [20, 52]. For this reason noise due to an additive fluctuating background is negligible. However, in measurements of the maximum intensity I_0, made with the particle attached to the glass wall, fluctuations in the intensity are nevertheless observed. In this study such measurements resulted in standard deviations of anywhere from 1.5 to 5 % of I_0. To capture this situation we use the BD simulation to

generate elevations h which are converted to intensities according to $I(t) = I_0(t)\exp(-\zeta h)$, where the incident intensity is represented by uncorrelated Gaussian noise with mean I_0 and standard deviation σ, just as previously done by Sholl et al. [28]. The potential used in the BD simulations consisted of the EDL repulsion and the gravitational terms of Eq. 9. Figure 6 shows some examples of potentials extracted from an analysis of the BD-generated data for the highest noise level considered, $\sigma/I_0 = 0.05$, for some different ionic strengths. One observes that while the large-distance part of the potentials is not too seriously affected, the decay of the shorter-range repulsion is in general not reproduced accurately in the presence of appreciable levels of noise in the incident intensity. As a consequence, an error in the screening length is introduced. In general, the error grows as the level of noise is increased. In addition, one sees in Fig. 6 that it increases as the ionic strength is increased. These effects are seen more readily in Fig. 7, where results for the extracted screening lengths from noise-distorted BD data are summarized as a function of ionic strength for noise levels that are relevant for the TIRM measurements in this work. From the results in Fig. 7, a precise screening length, say within the 2 nm reproducibility of a single measurement, can be achieved in the ionic strength range of Fig. 7 only when the fluctuations in the incident intensity are kept within about 3% of the mean incident intensity.

Referring to Fig. 5, where screening lengths from TIRM measurements in $MgSO_4$ and $ZnSO_4$ solutions are shown, analysis of the scattered intensity from the particles attached to the glass surface, made after completion of the measurement for the highest ionic strength in Fig. 5, resulted in $\sigma/I_0 \approx 0.04$ and 0.05 for $MgSO_4$ and $ZnSO_4$ solutions, respectively. As shown in Fig. 5, the screening lengths from the concentration series of $MgSO_4$ solutions agrees well with the curve from Fig. 7 corresponding to $\sigma/I_0 = 0.04$. The same holds for the screening lengths from the $ZnSO_4$ solutions at the higher ionic strengths, shortly after which the experimental I_0 and σ values were determined. Judging from the rather close correspondence between the extracted screening lengths and the Debye length for the lower $ZnSO_4$ ionic strengths, the measurements appear to have been conducted initially, at the lower ionic strengths, at a lower noise level than that reached by the end of the measurement series. It follows from these comparisons that we can attribute the difference between the calculated Debye lengths and screening lengths obtained from analysis of TIRM data to distortions caused by noise. Helden et al. [21], by suppressing the net van der Waals interaction, were able to reach ionic strengths in TIRM measurements as high as 200 mM. They observed that the screening lengths for higher ionic strengths were greater than the calculated Debye lengths, in agreement with the results of Fig. 7. At the highest salt concentrations they report a screening length that saturates at a value of 8.6 nm. Based on the trends in Fig. 7 the precise value is presumably dependent on the noise level, in line with the expectation that the maximum steepness that can be measured by TIRM is set by the decay length of the apparent potential extracted for the particle attached to the surface, as seen in Fig. 6.

4. Conclusions

The screened interactions between single colloidal spheres and a plane glass wall have been studied by TIRM. In agreement with findings from past TIRM

studies [20], van der Waals interactions determined by combining Lifshitz theory with Hamaker's geometrical factor for sphere-wall interactions or Derjaguin's approximation are found to be too strong compared to the interactions measured. The pair-wise additive approach of Suresh and Walz [38] furnishes expressions that take account of surface roughness, presumed to be the cause of the attenuation of the van der Waals interaction, while including both retardation and screening. TIRM measurements have been conducted in solutions of symmetric 1:1 and 2:2 electrolytes as well as asymmetric 2:1, 1:2, 3:1, and 3:2 electrolytes, including some surfactant solutions below their critical micelle concentrations. In all cases, except the 2:2 electrolytes, screening lengths, extracted by fitting TIRM-measured potentials, are found to agree with the Debye length to within about 2 nm. On the other hand, the 2:2 electrolytes, $MgSO_4$ and $ZnSO_4$, seem to yield less screening of the colloidal sphere-plane wall interaction than the corresponding Debye length. Although this trend is in qualitative agreement with theory, the measured deviation is substantially larger than what theory predicts for the salt concentrations examined. On the other hand, analysis of BD simulations with added noise in the incident intensity yields similar magnitudes for the deviation for realistic levels of noise. In the recent past, TIRM measurements were conducted in solutions with ionic strengths up to 10 mM and the deviations observed between screening lengths from those measurements and calculated Debye lengths were ascribed to subtle ion-specific effects [22]. The present study shows that special care need be taken to limit noise in the measurements at such high ionic strengths. Conceivably, post-processing by low-pass filtering techniques, as suggested by Odiachi and Prieve [53], might improve matters.

Acknowledgments

Financial support from the Swedish Research Council and the Swedish National Graduate School in Materials Science (NFSM) is gratefully acknowledged.

References

[1] J. Lyklema, Fundamentals of interface and colloid science, solid-liquid interfaces, II, Academic Press, London, 1995.

[2] D. F. Evans, H. Wennerström, The colloidal domain, 2nd Edition, Wiley-VCH, New York, 1999.

[3] L. Guldbrand, B. Jönsson, H. Wennerström, P. Linse, Electrical double-layer forces - a Monte Carlo study, J. Chem. Phys. 80 (1984) 2221-2228.

[4] J. N. Israelachvili, G. E. Adams, Measurement of forces between two mica surfaces in aqueous electrolyte solutions in the range 0-100 nm, J. Chem. Soc. Faraday Trans. 1 74 (1978) 975-1001.

[5] R. M. Pashley, J. N. Israelachvili, DLVO and hydration forces between mica surfaces in Mg2+, Ca2+, Sr2+, and Ba2+ chloride solutions, J. Colloid Interf. Sci. 97 (1984) 446-455.

[6] R. M. Pashley, Forces between mica surfaces in La3+ and Cr3+ electrolyte solutions, J. Colloid Interf. Sci. 102 (1984) 23-35.

[7] R. M. Pashley, B. W. Ninham, Double-layer forces in ionic micellar solutions, J. Phys. Chem. 91 (1987) 2902-2904.

[8] R. Tadmor, E. Hernández-Zapata, N. Chen, P. Pincus, J. N. Israelachvili, Debye Length and Double-Layer Forces in Polyelectrolyte Solutions, Macromolecules 35 (2002) 2380-2388.

[9] H.-J. Butt, B. Cappella, M. Kappl, Force measurements with the atomic force microscope: technique, interpretation and applications, Surf. Sci. Rep. 59 (2005) 1-152.

[10] D. C. Prieve, F. Luo, F. Lanni, Brownian motion of a hydrosol particle in a colloidal force field, Faraday Disc. Chem. Soc. 83 (1987) 297-307.

[11] J. Y. Walz, Measuring particle interactions with total internal reflection microscopy, Curr. Opin. Colloid Interf. Sci. 2 (1997) 600-606.

[12] D. C. Prieve, Measurement of colloidal forces with TIRM, Adv. Colloid Interf. Sci. 82 (1999) 93-125.

[13] H. H. von Grünberg, L. Helden, P. Leiderer, C. Bechinger, Measurement of surface charge densities on Brownian particles using total internal reflection microscopy, J. Chem. Phys. 114 (2001) 10094-10104.

[14] D. J. Mitchell, B. W. Ninham, Range of the screened Coulomb interaction in electrolytes and double layer problems, Chem. Phys. Lett. 53 (1978) 397-399.

[15] R. Kjellander, J. Mitchell, Dressed-ion theory for electrolyte solutions: A Debye-Huckel-like reformulation of the exact theory for the primitive model, J. Chem. Phys. 11 (1994) 603-626.

[16] M. A. Knackstedt, B. W. Ninham, Correlations and thermodynamic coefficients in dilute asymmetric electrolyte solutions, J. Phys. Chem. 100 (1996) 1330-1335.

[17] A. McBride, M. Kohonen, P. Attard, The screening length of charge-asymmtric electrolytes: a hypernetted chain calculation, J. Chem. Phys. 109 (1998) 2423-2428.

[18] Z. Abbas, M. Gunnarsson, E. Ahlberg, S. Nordholm, Corrected Debye-Hückel Analysis of Surface Complexation: I. Bulk Salt Limit, J. Colloid Interf. Sci. 243 (2001) 11-30.

[19] M. M. Kohonen, M. E. Karaman, R. M. Pashley, Debye length in multivalent electrolyte solutions, Langmuir 16 (2000) 5749-5753.

[20] M. A. Bevan, D. C. Prieve, Direct Measurement of Retarded van der Waals Attraction, Langmuir 15 (1999) 7925-7936.

[21] L. Helden, G. H. Koenderink, P. Leiderer, C. Bechinger, Depletion potentials induced by charged colloidal rods, Langmuir 20 (2004) 5662-5665.

[22] Z. Ao, G. Liu, G. Zhang, Ion Specificity at Low Salt Concentrations Investigated with Total Internal Reflection Microscopy, J. Phys. Chem. C 115 (2011) 2284-2289.

[23] A. Tulpar, V. Subramanian, W. Ducker, Decay lengths of double-layer forces in solutions of partly associated ions, Langmuir 17 (2001) 8451-8454.

[24] M. Nayeri, R. Karlsson, J. Bergenholtz, Surfactant effects on colloidal interactions: Concentrated micellar solutions of non-ionic surfactant, Colloids Surf. A 368 (2010) 84-90.

[25] S. G. Bike, Measuring colloidal forces using evanescent wave scattering, Curr. Opin. Colloid Interf. Sci. 5 (2000) 144-150.

[26] L. Helden, E. Eremina, N. Riefler, C. Hertlein, C. Bechinger, Y. Eremin, T. Wriedt, Single-particle evanescent light scattering simulations for total internal reflection microscopy, Appl. Opt. 45 (2006) 7299-7308.

[27] C. Hertlein, L. Helden, A. Gambassi, S. Dietrich, C. Bechinger, Direct measurement of critical Casimir forces, Nature 451 (2008) 172-175.

[28] D. S. Sholl, M. K. Fenwick, E. Atman, D. C. Prieve, Brownian dynamics simulation of the motion of a rigid sphere in a viscous fluid very near a wall, J. Chem. Phys. 113 (2000) 9268-9278.

[29] M. A. Bevan, D. C. Prieve, Hindered diffusion of colloidal particles very near to a wall: revisited, J. Chem. Phys. 113 (2000) 1228-1236.

[30] D. Maciejewska, A. Khan, B. Lindman, Magnesium and calcium surfactants: ternary phase diagrams of magnesium and calcium dodecyl-sulphate with decanol and water, Colloid Polym. Sci. 264 (1986) 909-916.

[31] J. Mahanty, B. W. Ninham, Dispersion forces, Academic Press, New York, 1976.

[32] B. A. Pailthorpe, W. B. Russel, The retarded van der Waals interaction between spheres, J. Colloid Interf. Sci. 89 (1982) 563-566.

[33] S. N. Thennadil, L. H. Garcia-Rubio, Approximations for calculating van der Waals interaction energy between spherical particles - a comparison, J. Colloid Interf. Sci. 243 (2001) 136-142.

[34] R. R. Dagastine, M. Bevan, L. R. White, D. C. Prieve, Calculation of van der Waals forces with diffuse coatings: Applications to roughness and adsorbed polymers, J. Adhesion 80 (2004) 365-394.

[35] L. Suresh, J. Y. Walz, Direct Measurement of the Effect of Surface Roughness on the Colloidal Forces between a Particle and Flat Plate, J. Colloid Interf. Sci. 196 (1997) 177-190.

[36] J. Y. Walz, L. Suresh, M. Piech, The effect of nanoscale roughness on long range interaction forces, J. Nanoparticle Res. 1 (1999) 99-113.

[37] J. Czarnecki, T. Dabros, Attenuation of the van der Waals attraction energy in the particle/semi-infinite system due to the roughness of the particle surface, J. Colloid Interf. Sci. 78 (1980) 25-30.

[38] L. Suresh, J. Y. Walz, Effect of Surface Roughness on the Interaction Energy between a Colloidal Sphere and a Flat Plate, J. Colloid Interf. Sci. 183 (1996) 199-213.

[39] J. H. Schenkel, J. A. Kitchener, A test of the Derjaguin-Verwey-Overbeek theory with a colloidal suspension, Trans. Faraday Soc. 56 (1960) 161-173.

[40] J. Gregory, Approximate expressions for retarded van der Waals interaction, J. Colloid Interf. Sci. 83 (1981) 138-145.

[41] H. C. Hamaker, The London-van der Waals attraction between

spherical particles, Physica 4 (1937) 1058-1072.

[42] J. Czarnecki, van der Waals attraction energy between sphere and half-space, J. Colloid Interf. Sci. 72 (1979) 361-362.

[43] D. Haughey, J. C. Earnshaw, Studies of colloidal interactions using total internal reflection microscopy, Colloids Surf. A 136 (1998) 217-230.

[44] W.-Y. Wen, S. Saito, C. Lee, Activity and Osmotic Coefficients of Four Symmetrical Tetraalkylammonium Fluorides in Aqueous Solutions at 25 degrees, J. Phys. Chem. 70 (1966) 1244-1248.

[45] S. Kusakabe, M. Arai, Solvent Extraction of Several Anions with Tetrabutylammonium Ion into 1,2-Dichloroethane and Hydration of Anions in the Organic Phase, Bull. Chem. Soc. Japan 69 (1996) 581-588.

[46] T. Ederth, P. M. Claesson, Forces between carboxylic acid surfaces in divalent electrolyte solutions, J. Colloid Interf. Sci. 229 (2000) 123-128.

[47] B. C. Donose, A. V. Nguyen, G. M. Evans, Y. Yan, Effect of aluminium sulphate on interactions between silica surfaces studied by atomic force microscopy, Water Res. 41 (2007) 3449-3457.

[48] P. L. Hayden, A. J. Rubin, Systematic investigation of the hydrolysis and precipitation of aluminum (iii), in: A. J. Rubin (Ed.), Aqueous-environmental chemistry of metals, Ann Arbor Science Publishers, Ann Arbor, MI, 1974, p. 317.

[49] J. Ulander, R. Kjellander, The decay of pair correlation functions in ionic fluids: a dressed ion theory analysis of Monte Carlo simulations, J. Chem. Phys. 114 (2001) 4893-4904.

[50] J. Ennis, R. Kjellander, D. J. Mitchell, Dressed ion theory for bulk symmetric electrolytes in the restricted primitive model, J. Chem. Phys. 102 (1995) 975-991.

[51] P. C. Odiachi, D. C. Prieve, Total internal reflection microscopy: distortion caused by additive noise, Ind. Eng. Chem. Res. 41 (2002) 478-485.

[52] D. Kleshchanok, Polymer-induced colloidal interaction: measured by direct and indirect methods, PhD thesis, Rheinisch-Westfälischen Technischen Hochschule Aachen, 2007.

[53] P. C. Odiachi, D. C. Prieve, Removing the effects of additive noise from TIRM measurements, J. Colloid Interf. Sci. 270 (2004) 113-122.